A Method to Improve the Semiquantification of ^{18}F-FDG Uptake: Reliability of the Estimated Lean Body Mass Using the Conventional, Low-Dose CT from PET/CT

Pierre Decazes[1–3], Denis Métivier[4], Alexandra Rouquette[5,6], Jean-Noël Talbot[1,7], and Khaldoun Kerrou[1]

[1]Department of Nuclear Medicine, Hôpital Tenon, APHP, Paris, France; [2]Department of Nuclear Medicine, Hôpital Cochin, APHP, Paris, France; [3]Université Paris-Descartes, Paris, France; [4]Department of Nuclear Medicine, HIA du Val-de-Grâce, Paris, France; [5]Biostatistic and Epidemiology Department, Hôtel-Dieu, APHP et Université Paris-Descartes, Paris, France; [6]Inserm, U1178, Mental Health and Public Health, Universités Paris-Sud and Paris-Descartes, Paris, France; and [7]Université Pierre et Marie Curie, Paris, France

The standardized uptake lean body mass (SUL), calculated using lean body mass (LBM), is essential for the semiquantification of ^{18}F-FDG uptake using PET coupled with CT to avoid a bias linked to the adipose mass. It allows the evaluation of a response to therapy according PERCIST 1.0. The aim of this study was to evaluate the reliability of a method for the estimation of the LBM using the data of the low-dose CT from PET/CT acquired over standard acquisition fields (from skull base to ischia, from vertex to ischia, from skull base to mid thigh, from vertex to mid thigh). **Methods:** We wrote an automated program that determined the LBM from a CT with limited fields of acquisition and applied this method in a large (184 patients) and heterogeneous population. Its results were compared with the measurement of LBM from whole-body CT (reference standard) and the results of 5 predictive equations described in the literature. **Results:** The results of LBM measurement evaluated with this technique were much closer to the reference standard than those obtained by the mathematic formulas. The intraclass correlations (ICC) of this technique compared with the reference standard were excellent (the best ICC being obtained for the largest acquisition field, from vertex to mid thigh: ICC, 0.994; 95% confidence interval [95% CI], 0.992–0.995; $P < 0.0001$), much better than the ICC obtained with the mathematic formulas (the best ICC for a mathematic formula was 0.841; 95% CI, 0.714–0.903; $P < 0.0001$). Moreover, the analysis with the Bland–Altman plot showed that the differences in mean lean masses between the studied technique and the reference standard was the smallest for the proposed technique (for the largest acquisition field, mean difference 0.2 kg with the narrowest 95% CI [−1.8 to 2.2 kg]). **Conclusion:** This technique could be easily implemented on computers used in practice to allow a more reliable assessment of the SUL in clinical practice notably for the therapeutic evaluations after PERCIST 1.0.

Key Words: positron-emission tomography; tomography; x-ray; ^{18}F-fluorodeoxyglucose; body fat distribution; lean body mass

J Nucl Med 2016; 57:753–758
DOI: 10.2967/jnumed.115.164913

The most widely used index for semiquantification of the uptake of ^{18}F-FDG using PET/CT is the SUV, defined as the ratio of the radioactive concentration measured in the region of interest (kBq/mL) over the activity injected into the patient (kBq) divided by the patient's volume (mL). In practice, assuming that the patient has a homogeneous mass density of 1 g/mL, the SUV is calculated using the weight of the patient in g rather than the body volume (*1*).

$$\mathrm{SUV} = \frac{\text{Radioactive concentration (kBq/mL)}}{\text{Activity injected (kBq)/weight (g)}}. \qquad \text{Eq. 1}$$

However, this assumption induces a bias because adipose tissue metabolizes far less ^{18}F-FDG than other tissues. So, for 2 patients of equal weight but with different fat mass, the SUV of the nonfatty tissues, including tumors, will be higher for the fattier patient (*2*).

To avoid such a bias, it is proposed to replace the weight in the SUV calculation by the lean body mass (LBM), defined by the weight subtracted by the body fat weight (*2,3*). This measurement is frequently referred to as SUL, L standing for lean body mass. The replacement of SUV by SUL has been endorsed by Wahl et al. for PERCIST 1.0, aiming to standardize the metabolic response of solid tumors to therapy based on ^{18}F-FDG uptake on PET/CT, especially for clinical trials (*4*).

To determine the type of response, PERCIST 1.0 introduces an evaluation of the relative and the absolute changes of the SUL of targets between pretreatment and posttreatment examinations. It is easy to demonstrate mathematically that, contrary to the absolute changes, the relative changes are not influenced by the LBM, even wrongly estimated, if it stays constant. However, cancer can modify the body composition (*5*), and therefore the LBM estimation may change between both examinations and influence the relative changes.

So an accurate SUL measurement requires a valid estimation of LBM. Its calculation by a mathematic formula from easily available characteristics of the patient (such as height and weight) is simple but may not be reliable enough to be used in practice (*6–8*). Many diagnostic tests have been proposed to measure LBM (*9–11*). One test is of notable interest: the whole-body CT (CT_{WB}). Indeed, CT is performed for each PET/CT examination. So, using data from this CT to measure LBM could give an accurate

Received Aug. 5, 2015; revision accepted Dec. 1, 2015.
For correspondence or reprints contact: Pierre Decazes, Department of Nuclear Medicine, Cochin Hospital, 27 rue du Faubourg Saint Jacques, 75679 Paris Cedex 14, France.
E-mail: pierre.decazes@parisdescartes.fr
Published online Dec. 30, 2015.

measure and would reduce study time for the patients, health care personnel, and medical equipment.

However, in most patients, the field of acquisition of the so-called whole-body PET/CT covers only the upper part of the body (from vertex to mid thigh). Considering this limited acquisition field, Chan proposed a technique to estimate the LBM of a patient from the data of the CT originating from only a part of the whole body and found, for 18 patients, a high paired-samples correlation coefficient (0.998 for a CT field from vertex to 20 cm below the ischia) between the result of his method and the LBM obtained from the CT_{WB} (*12*).

Nevertheless, these good results have to be confirmed because the sample size of this pilot study was small and the studied population quite homogeneous, particularly concerning the body mass index, without any patient having a body mass index higher than 30 kg/m^2. Moreover, no information concerning the extrapolation of the results in other populations was given, so this technique may not be able to be implemented in practice.

The main objective of our work was thus to evaluate the reliability of the Chan method for the estimation of the LBM using CT acquired from limited acquisition fields and on a large and representative sample with adapted statistical tools: intraclass correlation coefficients (ICCs) and Bland–Altman plots (*13–15*).

Our secondary objective was to evaluate the reliability of LBMs estimated using 5 mathematic formulas based on the subjects' characteristics such as weight, height, sex, or body mass index (*16–18*).

MATERIALS AND METHODS

Data Acquisitions

The Committee for the Protection of People "Ile-de-France V" approved this retrospective study, and the requirement to obtain informed consent was waived.

PET/CT scans were acquired over the full body (from vertex to toes) with different PET tracers (^{18}F-FDG, ^{18}F-fluoride, ^{18}F-fluoroDOPA, and ^{68}Ga-DOTATOC) in patients older than 18 y from November 1, 2012, to October 31, 2013, at the nuclear medicine department of Hôpital Tenon in Paris. All examinations were performed on a GEMINI TF scanner (Philips) with a 16-slice CT component. The acquisition parameters for the low-dose CT were 120 kVp and 76–80 mAs (adapted to 100–120 mAs for some obese patients). The pixel size was 1.172 × 1.172 mm^2 (or voxels of 3.433 mm^3 for a slice thickness of 2.5 mm) or, when the field of view was enlarged for obese people, 1.367 × 1.367 mm^2 (or voxels of 4.673 mm^3 for a slice thickness of 2.5 mm).

Image Processing

CT data were processed using ImageJ software (version 1.48 d; National Institutes of Health) (*19*). The operator checked the absence of exclusion criteria on the CT (not a full-body acquisition, arms above head, important artifacts, pathology significantly modifying the distribution of fat) and determined the reference slices including landmarks, which were used for measurement (the distal end of the body, ischia, eyes, and vertex).

Fat segmentation was performed as follows. The aim was to select every fat voxel by windowing using densities of the fat tissues of −190 and −30 Hounsfield units (HUs) (*10,20*). Because voxels from some extra-body elements had a density included in this range of HUs, the body voxels were automatically isolated using a plug-in written for the ImageJ software with a threshold (−350 HU) to generate a binary image, keeping all the intrabody voxels and eliminating most of the extra-body voxels (mainly air); a morphologic open function to erase most of the table voxels; a rectangular mask automatically localized to eliminate the few remaining table voxels below the head; a « fill holes » function to fulfill the intrabody air voxels; a median filtering to eliminate the remaining extra-body voxels; and an inversion with a conversion to a 16 bits encoding to get a body mask (body voxels value set at 0 and the extra-body voxels at 65,534). The body voxels were thus isolated using this body mask subtracted from the original 16-bit CTs, and the windowing (from −190 to −30 HU) was then applied to isolate the fat voxels. The operator visually checked the quality of the insulation of the pixels of fat on a slice-by-slice basis.

Measurements

The reference standard used in this study was the LBM computed using data from the CT_{WB} (LBM_{WB}):

$$LBM_{WB}(g) = W(g) - BFM_{WB}(g), \quad \text{Eq. 2}$$

with $W(g)$ the subject's weight in g measured by a weighting scale and $BFM_{WB}(g)$ the body fat mass in g measured on the CT_{WB} and computed as:

$$BFM_{WB}(g) = \sum Fatvoxels_{vertex\text{-}toe} \times volume_{voxel}(mL) \times density_{fat}(g/mL), \quad \text{Eq. 3}$$

with $\sum Fatvoxels_{vertex\text{-}toe}$ the number of fat voxels in the whole body, $volume_{voxel}(mL)$ the volume of 1 voxel, and $density_{fat}$ the volumic mass density of fat equal to 0.923 g/mL (*10*).

The LBM was estimated from the CT with 4 different limited acquisition fields, the LBM of the missing parts of the body being extrapolated: LBM_{VI} from vertex to the ischia, LBM_{EI} from the eyes (corresponding to the skull base) to the ischia, LBM_{E20} from the eyes to 20 cm below the ischia (corresponding to the mid thigh), and LBM_{V20} from vertex to 20 cm below the ischia. By definition LBM_{V20} (with an adaptation of the formula for LBM_{EI}, LBM_{VI}, and LBM_{E20} with the respective data) was:

$$LBM_{V20}(g) = W(g) - \frac{BFM_{V20}(g) \times 100}{\%BFM_{V20}}, \quad \text{Eq. 4}$$

with $BFM_{V20}(g)$ the body fat mass in g measured on the CT with a limited acquisition field and computed as:

$$BFM_{V20} = \sum Fatvoxels_{vertex\text{-}20cm} \times volume_{voxel}(mL) \times density_{fat}(g/mL), \quad \text{Eq. 5}$$

with $\sum Fatvoxels_{vertex\text{-}20\ cm}$ the number of fat voxels in the part of the body (from vertex to 20 cm below the ischia), and $\%BFM_{V20}$ the percentage of the whole BFM located between the vertex and 20 cm below the ischia, theoretically computed as:

$$\%BFM_{V20} = \frac{BFM_{V20} \times 100}{BFM_{WB}}. \quad \text{Eq. 6}$$

Because, in practice, the BFM_{WB} of the subject will not be available to compute $\%BFM_{V20}$, the mean of $\%BFM_{V20}$ computed on the whole population was used in Equation 4.

The secondary objective was to compare the results of our technique with LBMs calculated using 5 predictive equations: LBM_{F1}, LBM_{F2}, LBM_{F3}, LBM_{F4}, and LBM_{F5} (Table 1).

Statistics

Continuous variables were reported as mean ± SD and categoric ones as frequencies (percentage). Agreement between the 9 outcomes

TABLE 1
Predictive Equations Evaluated with Weight, Height, Age, Sex, and Body Mass Index

Predictive equation	Reference
LBM_{F1}	*16,24*
Man $= 0.32810 \times W + 0.33929 \times H - 29.5336$	
Woman $= 0.29569 \times W + 0.41813 \times H - 43.2933$	
LBM_{F2}	*2*
Man $= 48 + 1.06 \times (H - 152)$	
Woman $= 45.5 + 0.91 \times (H - 152)$	
LBM_{F3}	*3,17*
Man $= 1.1 \times W - 120 \times (W/H)^2$	
Woman $= 1.07 \times H - 148 \times (W/H)^2$	
$LBM_{F4} = W - (W \times (1.2 \times BMI + (0.23 \times A) - 10.8 \times S - 5.4)/100)$	*25*
$LBM_{F5} = W - (W \times (76.0 - 1097.8 \times (H^2/W) + 0.053 \times A)/100)$	*6,18*

Weight, kg (W); height, cm (H); age, years (A); sex (S), coded 0 for woman and 1 for man; body mass index, kg/m^2 (BMI).

and the reference standard (LBM_{WB}) was estimated by means of the ICC (*13*). Bland–Altman plots (*14*) were also constructed to offer a graphical representation of the agreement between the 9 estimated LBMs and the reference standard. The hypothesis of the normality of the distribution of values, required to compute the ICCs and to interpret the Bland–Altman plots, was graphically checked.

Furthermore, 2 clinically relevant illustrations of those results were performed. First, using the mean weight and the mean LBM_{WB} in the whole sample, the SUL_{WB} was computed for the discrete arbitrary SUV of 5. Then, the corresponding SULs and their relative variations were calculated according to the 9 studied techniques using the results visualized on the Bland–Altman plots, to calculate LBMs: the mean difference between each of these LBMs and LBM_{WB} and their 95% confidence intervals (CIs). Second, the reference diagram of response according to PERCIST was drawn for pretreatment and posttreatment SULs varying from 0 to 10 units. As recommended in PERCIST 1.0, a partial metabolic response was defined as a ΔSUL lower than −30% and a decrease of at least 0.8 unit of SUL, a progressive metabolic disease as a ΔSUL greater than 30% and an increase of at least 0.8 unit of SUL, and finally a stable metabolic disease as the response between these 2. From the mean variations of SULs and their CIs obtained in the first clinically relevant illustration, the response diagrams according to PERCIST were then drawn for the 9 techniques, the CI being obtained by the combination of the low estimated SUL for the pretreatment PET/CT and the high estimated SUL for the posttreatment PET/CT (and inversely).

Statistical analyses were performed with the software R (version 3.1.3) (*21*).

RESULTS

Population

Over the inclusion period, 199 cases met the inclusion criteria but 15 cases were excluded because CT scanning was performed in 3 patients with pathologies altering the fat distribution (major edema of the lower limbs and liposarcoma) and in 3 patients with arms above the head, and 9 scans were duplicates. Characteristics of the 184 patients of the sample are described in Table 2.

Mean, ICC, and Bland–Altman Plot

The mean %BFMs in the whole sample and used in Equation 4 to compute LBM_{EI}, LBM_{VI}, LBM_{E20}, and LBM_{V20} were, respectively, $\%BFM_{EI} = 70.9\%$ (±6.8), $\%BFM_{VI} = 71.6\%$ (±6.7), $\%BFM_{E20} = 86.0\%$ (±3.9), and $\%BFM_{V20} = 86.7\%$ (±3.8). The distribution of each of the 9 estimated LBMs was considered graphically as corresponding to a normal distribution. Their mean and their ICCs computed using LBM_{WB} as the reference standard are shown on Table 3. The agreements of LBM_{EI}, LBM_{VI}, LBM_{E20}, and LBM_{V20} with LBM_{WB} were excellent, with a lower bound of the 95% CI of the ICC higher than 0.95, distinct from the ICC of the other estimated LBMs.

Bland–Altman plots for each of these estimated LBMs are shown in Figure 1. LBM_{V20} exhibited the strongest agreement

TABLE 2
Description of Population

Characteristic	Mean ± SD, unless otherwise stated	Radioactive tracer	Frequency (%)	Pathology	Frequency (%)
Age (y)	61.2 ± 14.6 (range, 20–90)	^{18}F-FDG	134 (73%)	Cancers	134 (73%)
Height (m)	1.69 ± 0.09 (range, 1.48–1.85)	^{18}F-fluoride	46 (25%)	Infectious diseases	25 (13.5%)
Weight (kg)	72.7 ± 15.2 (range, 39–118)	^{18}F-fluoroDOPA	1 (0.5%)	Inflammatory diseases	13 (7%)
Body mass index (kg/m^2)	25.4 ± 10.4 (range, 14.5–41.8)	^{68}Ga-DOTATOC	3 (1.5%)	Others	12 (6.5%)
Sex (%)	Men, 117 (64%)	Total	184 (100%)	Total	184 (100%)

TABLE 3
Mean, SD, and ICC of LBM Computed Using 9 Studied Techniques with LBM_{WB} as Reference Standard

Tested	Mean ± SD (kg)	ICC compared with LBM_{WB}	*P*
LBM_{F1}	50.5 ± 7.9	0.762 (0.297–0.893)	0.0021
LBM_{F2}	64.6 ± 10.6	0.3 (0–0.662)	0.151
LBM_{F3}	54.6 ± 10.2	0.629 (0–0.865)	0.056
LBM_{F4}	48.7 ± 9.7	0.841 (0.714–0.903)	<0.0001
LBM_{F5}	46.5 ± 5.6	0.748 (0.676–0.805)	<0.0001
LBM_{EI}	45.9 ± 9.1	0.964 (0.952–0.973)	<0.0001
LBM_{VI}	45.9 ± 9.1	0.967 (0.956–0.975)	<0.0001
LBM_{E20}	46.0 ± 9.4	0.992 (0.988–0.995)	<0.0001
LBM_{V20}	46.0 ± 9.4	0.994 (0.992–0.995)	<0.0001
LBM_{WB}	46.3 ± 9.4		

Data in parentheses are 95% CIs.

with LBM_{WB}, with the closest mean (+0.2 kg) to LBM_{WB} mean and the narrowest 95% CI (−1.8; + 2.2 kg) and no bias (flat regression line).

Illustrations

In our sample, the average weight was 72.7 ±15.2 kg, and the average LBM_{WB} was 46.3 ±9.4 kg. For this hypothetic average individual and an SUV arbitrarily set at 5, the computed SUL_{WB} was 3.18. Table 4 shows the average SULs (and their 95% CIs) computed using the results visualized on the Bland–Altman plots and their relative variations compared with the SUL_{WB}. The SUL computed with the LBM_{V20} was the closest to the SUL_{WB}, with the narrowest CI.

In Figure 2, showing the response according to PERCIST depending on the LBM estimated by the 9 studied techniques to calculate the SUL, 2 main results were observed. First, plain black lines separating the different types of response calculated using the mean variations of SULs for each technique varied slightly depending on the 9 techniques, with only a notable difference observed for LBM_{F2} for the low SULs (SULs < 2.67). Second, the CI areas of these lines were large for the mathematic formulas, with even an overlapping of these areas, and narrow for the techniques using a CT (the narrowest areas being obtained for the 2 largest fields of acquisitions).

DISCUSSION

In our study, we have shown on a large and heterogeneous population that the LBMs extrapolated from the data of a CT with a limited field of acquisition had an excellent agreement with the LBM measured using a CT_{WB}. Moreover, the Bland–Altman plots also showed that the mean differences between LBM_{WB} and the LBMs extrapolated from the data of a CT were small, with a narrow CI when the fields of acquisition were large (vertex or eyes to 20 cm below the ischia) and without bias. When the field of acquisition was smaller (vertex or eyes to the ischia), larger CIs were observed in the Bland–Altman plot and this can probably be explained by the fact that the zone between the ischia and 20 cm below is highly variable between patients. In his sample of 18 patients, Chan found a high paired-samples correlation coefficient of 0.998 between LBM_{V20} and the LBM measured using a CT_{WB} and also high correlation coefficients when other fields of acquisition were evaluated (*12*). Our results confirmed his findings. This is also consistent with the findings of Hamill et al. (*22*) who introduced 2 novel techniques for defining SUV based on CTs with limited field of acquisition while accounting for the patient habitus. However, the assumption used by Hamill et al. to extrapolate the LBM of the missing part of the body was different from the one used by Chan. Hamill et al. hypothesized, notably for their first technique, that the relative distributions of fat, lean, and bone in the scanned regions were the same whatever the part of the body, whereas Chan hypothesized that the distribution of the fat tissues was identical for all patients but could vary between the different parts of the body. We have confirmed in our study the relevance of the hypothesis of Chan to measure the LBM by comparing his technique to a validated reference standard. In their study, Hamill et al. used the body weight as the reference standard by comparing the CT_{WB}-based mass estimate with the body weight for some pigs and for 19 patients, which could have led to biased comparisons when LBM is strictly considered.

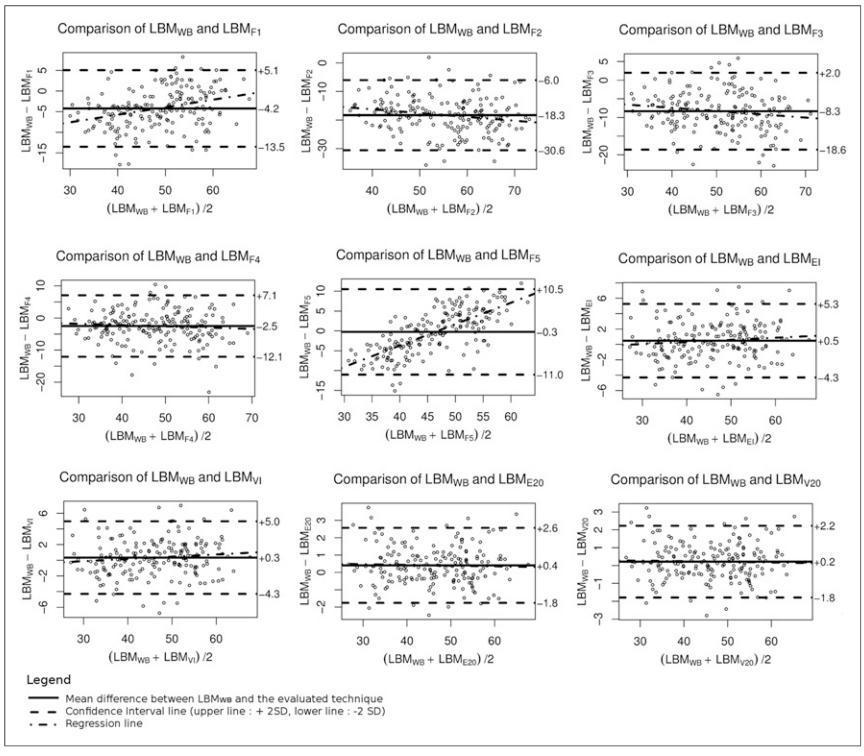

FIGURE 1. Bland–Altman plots of LBM computed using 9 studied techniques with LBM_{WB} as reference standard.

TABLE 4
SUL Calculated for SUVs Arbitrarily Fixed at 5 with Average Weight in This Study and Results of LBM Computed Using 9 Studied Techniques

Studied technique	SUL calculated for SUV = 5	Relative variations of SUL from reference SULs (%)
LBM_{F1}	3.47 (2.83–4.11)	9% (–11% to 29%)
LBM_{F2}	4.44 (3.59–5.28)	40% (13% to 66%)
LBM_{F3}	3.35 (3.04–4.46)	18% (–4% to 40%)
LBM_{F4}	3.35 (2.69–4.01)	5% (−15% to 26%)
LBM_{F5}	3.20 (2.46–3.94)	0.6% (−22% to 24%)
LBM_{EI}	3.15 (2.82–3.48)	−0.9% (−11% to 9%)
LBM_{VI}	3.16 (2.84–3.47)	−0.6% (−11% to 9%)
LBM_{E20}	3.15 (3.00–3.30)	−0.9% (−6% to 4%)
LBM_{V20}	3.17 (3.03–3.30)	−0.3% (−5% to 4%)
LBM_{WB}	3.18	0%

Data in parentheses are 95% CIs. Variations of these SULs from respective reference SUL calculated with LBM_{WB}.

Concerning the secondary objective of our study, the evaluation of the reliability of LBMs estimated using 5 mathematic formulas, we found that the predictive equations were unsuitable to accurately estimate the LBM. This finding confirmed the results of the study of Erselcan et al. (*6*) who demonstrated in a sample of 153 patients, using the dual-energy x-ray absorptiometry as the reference standard, the inadequacy of these mathematic formulas to estimate the LBM and therefore the SUL. However, 1 of the predictive equations, LBM_{F5}, had quite interesting results in his study, with a nonsignificant difference between the mean LBM_{F5} and the mean value of the reference standard, using a paired *t* test. In our study, we have also shown with the Bland–Altman plot of LBM_{F5} that the mean difference between LBM_{F5} and LBM_{WB} was small, but there was a high imprecision with a large CI and, more preoccupying, there was a bias function of the patient's weight (overestimation for the leanest patients and underestimation for the fattier patients). In 2 studies, Kim et al. also showed the discrepancies between the LBM estimated by predictive equations and by limited-field-of-acquisition CT (*7*) and by CT_{WB} (*8*). However, in those studies, no extrapolation of the data contained in the missing fields was performed when the field of acquisition was limited.

In our clinically relevant illustration, the variation of the SUL computed using LBM_{V20} was only −0.3% (95% CI, −5% to 4%), which is compatible with a good precision of the estimated SUL. In the illustration of the consequences on PERCIST 1.0, the absence of a clear difference between the lines separating the different types of response obtained with all the evaluated techniques and the reference lines led us to surmise that the response evaluation is not modified by the technique used to estimate the LBM if this LBM is stable between the pretreatment and posttreatment PET/CT (even wrongly estimated). However, large CI areas of these lines were observed with the mathematic formulas. The observation suggests that the LBM changes could lead to an inaccurate therapeutic response evaluation when a low estimated LBM used for the pretreatment PET/CT is combined to a high estimated LBM used for the posttreatment PET/CT (and inversely). On the contrary, the CI areas were narrow for the techniques using the largest fields of acquisition (LBM_{E20} and LBM_{V20}), suggesting that this evaluation would be close to the one obtained using the reference standard LBM from the CT_{WB}. The effect of the body modification on therapeutic evaluation has already been observed in a study comparing various SUV normalizations (body weight, body surface area, LBM, ideal body weight) and in which weight loss during therapy was found to affect PERCIST response classification (*23*).

The program written for our study to measure the LBM on the CTs differs slightly from the one described by Chan (*12*). In particular, a manual detection by the operator of the reference slices containing landmarks was favored in our work considering that when this program is applied in clinical practice to a PET/CT with a limited field of acquisition, no reference slice is searched. Interestingly, the program written for our study was fully automated for the measurement of the LBM for a determined field of acquisition and can therefore, if combined

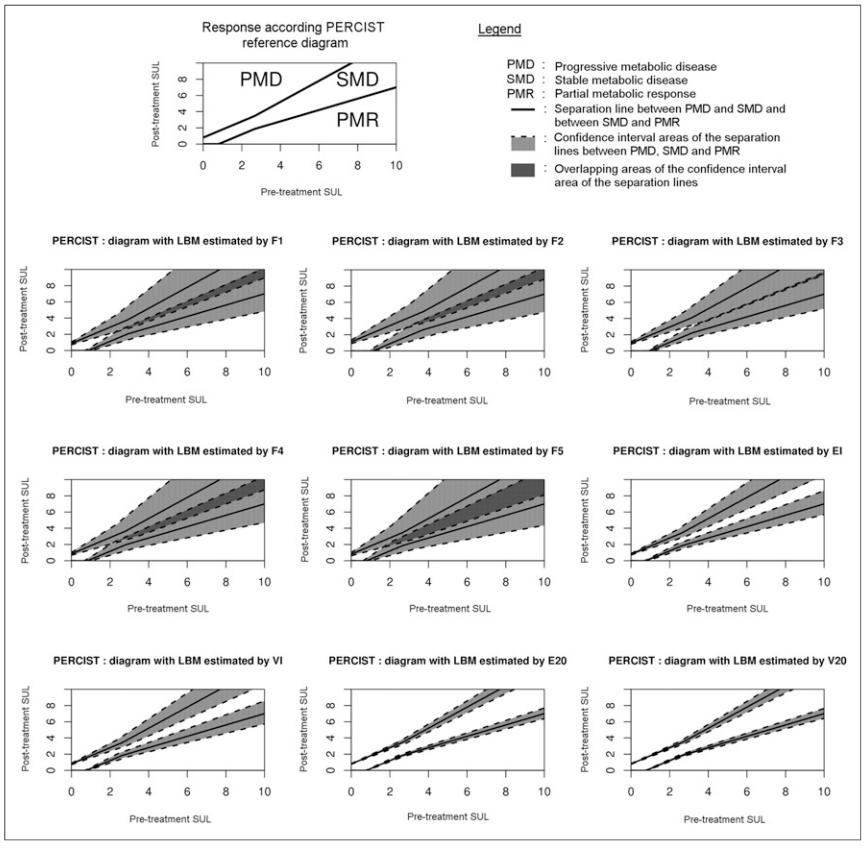

FIGURE 2. Diagrams illustrating response according PERCIST in function LBM computed using 9 studied techniques, with results obtained by Bland–Altman plot.

with the result of the adequate %BFM, be implemented in the clinic routinely. However, we must stress that the removal of the examination table is dependent of the type used by the manufacturer and this part has to be eventually adapted. Another difference between the Chan technique and ours was that Chan had systematically withdrawn the studied patient from the sample to define %BFM before using the mean of %BFMv20 in Equation 4, arguing that it could introduce a bias. Indeed, in such a small sample (18 patients), this technique seemed interesting but in our study, because our sample was larger, we decided to use the mean %BFM of the whole sample in function of the field of acquisition analyzed (respectively, $\%BFM_{EI}$, $\%BFM_{VI}$, $\%BFM_{E20}$, and BFM_{V20}).

Concerning the determination of the LBM with the CT data, we suggest that it is easier to measure the BFM and then subtract it from the body weight than to measure directly the LBM because the fat voxels correspond to a well-defined peak on the CT histogram with known lower and maximum HU densities and known mass density (*10*). Because the fat peak is well defined on the CT histogram and quite large (from −190 to −30 HU), the results depend little on the image noise, and therefore, the absence in general of adaptation of the CT parameters in function of the morphology (only 3 obese patients had the exposure increased to 100–120 mAs) does not compromise the estimation of the BFM in our study.

Finally, in our study, the arms of the patient were put along the body whereas, usually, they are maintained above the head when PET/CT with a limited field of acquisition is performed. This difference would not compromise the estimation of LBM with the studied technique if the arms are in the field of acquisition of the CT. Moreover, when the arms are along the body, they can be partly outside the field of view and so slightly modify the measure of LBM. This case has been limited in our study because the fields of view were enlarged if needed.

CONCLUSION

The SUL is recommended, according to the PERCIST 1.0 (*4*), to replace the SUV for therapy response evaluation of solid tumors by PET/CT. In 2012, Chan (*12*) defined a technique to estimate the LBM from a CT with a limited field of acquisition. In our study, we have confirmed the reliability of the Chan technique from data of a larger and more heterogeneous sample of patients. This technique is particularly interesting in nuclear medicine because it uses already existing information, avoiding an additional cost in time, personnel, money, and, potentially, radiation exposure.

DISCLOSURE

The costs of publication of this article were defrayed in part by the payment of page charges. Therefore, and solely to indicate this fact, this article is hereby marked "advertisement" in accordance with 18 USC section 1734. No potential conflict of interest relevant to this article was reported.

REFERENCES

1. Buvat I. Les limites du SUV. *Med Nucl (Paris).* 2007;31:165–172.
2. Zasadny KR, Wahl RL. Standardized uptake values of normal tissues at PET with 2-[fluorine-18]-fluoro-2-deoxy-D-glucose: variations with body weight and a method for correction. *Radiology.* 1993;189:847–850.
3. Sugawara Y, Zasadny KR, Neuhoff AW, Wahl RL. Reevaluation of the standardized uptake value for FDG: variations with body weight and methods for correction. *Radiology.* 1999;213:521–525.
4. Wahl RL, Jacene H, Kasamon Y, Lodge MA. From RECIST to PERCIST: evolving considerations for PET response criteria in solid tumors. *J Nucl Med.* 2009;50(suppl 1):122S–150S.
5. Craig AB, Waterhouse C. Body-composition changes in patients with advanced. *Cancer.* 1957;10:1106–1109.
6. Erselcan T, Turgut B, Dogan D, Ozdemir S. Lean body mass-based standardized uptake value, derived from a predictive equation, might be misleading in PET studies. *Eur J Nucl Med Mol Imaging.* 2002;29:1630–1638.
7. Kim WH, Kim CG, Kim D-W. Comparison of SUVs normalized by lean body mass determined by CT with those normalized by lean body mass estimated by predictive equations in normal tissues. *Nucl Med Mol Imaging.* 2012;46:182–188.
8. Kim CG, Kim WH, Kim MH, Kim D-W. Direct determination of lean body mass by CT in F-18 FDG PET/CT studies: comparison with estimates using predictive equations. *Nucl Med Mol Imaging.* 2013;47:98–103.
9. Fogelholm M, van Marken Lichtenbelt W. Comparison of body composition methods: a literature analysis. *Eur J Clin Nutr.* 1997;51:495–503.
10. Chowdhury B, Sjöström L, Alpsten M, Kostanty J, Kvist H, Löfgren R. A multicompartment body composition technique based on computerized tomography. *Int J Obes Relat Metab Disord.* 1994;18:219–234.
11. Kullberg J, Brandberg J, Angelhed J-E, et al. Whole-body adipose tissue analysis: comparison of MRI, CT and dual energy X-ray absorptiometry. *Br J Radiol.* 2009;82:123–130.
12. Chan T. Computerized method for automatic evaluation of lean body mass from PET/CT: comparison with predictive equations. *J Nucl Med.* 2012;53:130–137.
13. Lee J, Koh D, Ong CN. Statistical evaluation of agreement between two methods for measuring a quantitative variable. *Comput Biol Med.* 1989;19:61–70.
14. Bland JM, Altman DG. Statistical methods for assessing agreement between two methods of clinical measurement. *Lancet.* 1986;1:307–310.
15. Altman DG, Bland JM. Statistics notes: the normal distribution. *BMJ.* 1995;310:298.
16. Hume R. Prediction of lean body mass from height and weight. *J Clin Pathol.* 1966;19:389–391.
17. James W. Research on obesity, a report of the DHSS/MRC group. *Her Majesty's Station Off Lond.* 1976.
18. Gallagher D, Heymsfield SB, Heo M, Jebb SA, Murgatroyd PR, Sakamoto Y. Healthy percentage body fat ranges: an approach for developing guidelines based on body mass index. *Am J Clin Nutr.* 2000;72:694–701.
19. Schneider CA, Rasband WS, Eliceiri KW. NIH Image to ImageJ: 25 years of image analysis. *Nat Methods.* 2012;9:671–675.
20. Kvist H, Sjöström L, Tylén U. Adipose tissue volume determinations in women by computed tomography: technical considerations. *Int J Obes.* 1986;10:53–67.
21. *R: A Language and Environment for Statistical Computing*. The R Foundation website. http://www.R-project.org. Accessed February 26, 2016.
22. Hamill JJ, Sunderland JJ, Leblanc AK, Kojima CJ, Wall J, Martin EB. Evaluation of CT-based lean-body SUV. *Med Phys.* 2013;40:092504.
23. Shields A, Wilson A, Narayanan M, et al. Does PERCIST normalized for body surface area, body weight, or ideal body weight equal PERCIST normalized for lean body mass? *J Nucl Med.* 2012;53(suppl 1):1338.
24. Velasquez LM, Boellaard R, Kollia G, et al. Repeatability of ^{18}F-FDG PET in a multicenter phase I study of patients with advanced gastrointestinal malignancies. *J Nucl Med.* 2009;50:1646–1654.
25. Pieterman R, Willemsen A, Appel M, et al. Visualisation and assessment of the protein synthesis rate of lung cancer using carbon-11 tyrosine and positron emission tomography. *Eur J Nucl Med Mol Imaging.* 2002;29:243–247.